Melatonin-induced miR-181c-5p enhances osteogenic differentiation and mineralization of human jawbone-derived osteoblastic cells

HIROSHI MURODUMI[1], HIDEO SHIGEISHI[2], HIROKI KATO[1], SHO YOKOYAMA[1], MIYUKI SAKUMA[1], MISATO TADA[1], SHIGEHIRO ONO[1], MOHAMMAD ZESHAAN RAHMAN[3], KOUJI OHTA[2] and MASAAKI TAKECHI[1]

Departments of [1]Oral and Maxillofacial Surgery and [2]Public Oral Health, Graduate School of Biomedical and Health Sciences, Hiroshima University, Hiroshima 734-8553, Japan; [3]Department of Oral and Maxillofacial Surgery, Pioneer Dental College and Hospital, Joar Sahara, Baridhara, Dhaka 1229, Bangladesh

Received September 23, 2019; Accepted June 22, 2020

DOI: 10.3892/mmr.2020.11401

Abstract. Our previous study revealed that treatment with a combination of fibroblast growth factor-2 and melatonin (MEL) synergistically augmented osteogenic activity and mineralization of MC3T3-E1 mouse preosteoblast cells. Thus, the objective of the present study was to assess the effect of MEL on osteogenetic characteristics in human osteoblastic cells. Human jawbone-derived osteoblastic (hOB) cells were isolated from mandibular bone fragments. RUNX family transcription factor 2 (Runx2) expression, alkaline phosphatase (ALP) enzyme activity and the mineralization ability of hOB cells in the presence of MEL were evaluated. Microarray analysis was also performed to assess the expression of MEL-induced microRNAs (miRNAs/miRs) in hOB cells. Treatment with MEL significantly enhanced Runx2 expression, ALP activity and mineralization staining. However, this effect was significantly reduced following transforming growth factor-β1 treatment. In total, 124 miRNAs were differentially expressed in MEL-treated hOB cells, compared with untreated cells. Of the upregulated miRNAs, miR-181c-5p exhibited the largest fold change. Runx2 mRNA expression and mineralization staining in the presence of MEL were significantly reduced following transfection with a miR-181c-5p inhibitor. In addition, transfection with miR-181c-5p mimics significantly increased Runx2 expression and mineralization staining. These results suggested that MEL-induced miR-181c-5p was involved in osteogenic differentiation and mineralization of hOB cells. Using TargetScan, a putative miR-181c-5p binding site was identified in the Notch2 gene. Moreover, Notch2 mRNA and protein expression levels in hOB cells were significantly reduced following transfection with miR-181c-5p mimics, confirming Notch2 as a target gene for miR-181c-5p. Notch2 siRNA knockdown significantly increased Runx2 expression and mineralization staining, which suggested that Notch2 may negatively regulate osteogenic differentiation of hOB cells by downregulating Runx2. In conclusion, MEL-induced expression of miR-181c-5p enhanced osteogenic differentiation and calcification of hOB cells.

Correspondence to: Dr Hideo Shigeishi, Department of Public Oral Health, Graduate School of Biomedical and Health Sciences, Hiroshima University, 1-2-3 Kasumi, Minami-ku, Hiroshima 734-8553, Japan
E-mail: shige@hiroshima-u.ac.jp

Abbreviations: MEL, melatonin; ALP, alkaline phosphatase; miRNA/miR, microRNA

Key words: human osteoblastic cells, mineralization, melatonin, RUNX family transcription factor 2, miR-181c-5p

Introduction

Melatonin (MEL) is a hormone that is primarily synthesized and secreted by the pineal gland, but also by other organs, including the retina, testes, Harderian gland, bone marrow and gastrointestinal tract (1-4). Moreover, MEL has various functions, such as circadian rhythm regulation, sleep promotion, neuroprotection, tumor suppression and hormone release regulation (5). With respect to bone metabolism, MEL promotes human mesenchymal stem cell and preosteoblast cell differentiation, as well as attenuates receptor activator of NF-κB ligand-induced bone resorption (6-8). Our previous study revealed that MEL was involved in osseointegration around titanium implants in rat models (9). In addition, treatment with a combination of fibroblast growth factor-2 and MEL synergistically augments osteogenic activity and mineralization of MC3T3-E1 mouse preosteoblast cells cultured with interconnected porous hydroxyapatite ceramics (10). MEL treatment also enhances osteoblastic differentiation and mineralization in MC3T3-E1 cells via bone morphogenic protein (BMP)/ERK/Wnt signaling pathways (11). These findings suggested that MEL serves an important role in osteoblast differentiation and mineralization.

The transforming growth factor-β (TGF-β)/Smad signaling pathway serves an essential role in osteoblastic cell differentiation and mineralization, as well as in skeletal development (12). In addition, TGF-β activation of the mitogen-activated protein kinase (MAPK)/ERK pathway is suggested to be involved in the regulation of osteoblastic cell differentiation (13). However, the relationship between MEL-induced osteoblastic cell differentiation and TGF-β activation of the MAPK/ERK signaling pathway remains unknown (10,13). microRNAs (miRNAs/miRs) are small non-coding RNAs that play a vital role in regulation of biological process, including osteoblastic differentiation (14). However, the role of MEL-induced miRNAs in osteogenic differentiation remains to be elucidated. Therefore, the aim of the present study was to evaluate the role of MEL in mineralization and the effect of TGF-β on osteoblastic cell differentiation in human jawbone-derived osteoblastic (hOB) cells. The association between MEL-induced miRNA and RUNX family transcription factor 2 (Runx2) was also examined.

Materials and methods

Cell culture. The present study protocol was approved by the Institutional Review Board of Hiroshima University. Fragments of mandibular ramus were obtained from a female patient in her 20s who underwent mandibular osteotomy in August 2017 and provided written informed consent for the use of the fragments in this study. hOB cells were isolated from the mandibular bone fragments using the following explant culture technique. Bone fragments were washed, minced in PBS, then plated in 60-mm culture dishes containing α-minimal essential medium (Sigma-Aldrich; Merck KGaA) supplemented with 10% FBS (Biological Industries), and 1% penicillin-streptomycin (Sigma-Aldrich; Merck KGaA) and incubated at 37˚C with 5% CO_2. When cells had grown to semi-confluence around the bone tissue, they were passaged with 0.025% trypsin (Gibco; Thermo Fisher Scientific, Inc.) and 0.02% EDTA (Gibco; Thermo Fisher Scientific, Inc.) in PBS Cells from passage 3-6 were used in the present study. Passaged hOB cells were cultured in the aforementioned medium.

hOB cells were cultured under 5% CO_2 in air at 37˚C. To enable differentiation of hOB cells, osteogenic medium with 10 nM dexamethasone, 10 mM β-glycerophosphate and 50 μg/ml ascorbic acid (all from Sigma-Aldrich; Merck KGaA) was used. hOB cells were cultured for 2 weeks under 5% CO_2 in air at 37˚C. In a preliminary experiment, hOB cells were treated with MEL (Sigma-Aldrich; Merck KGaA) at concentrations of 0.2, 1.0 and 2.0 μM for 2 weeks at 37˚C to determine the optimal concentration required. Recombinant human TGF-β1 (R&D Systems, Inc.) was used at a final concentration of 5.0 ng/ml. 10 μM LY2157299 (Selleck Chemicals) was used as a TGF-β receptor inhibitor. 1.0 μM LY3214996 (Selleck Chemicals) was used as a selective ERK1/2 inhibitor. hOB cells were treated with TGF-β1, LY2157299 or LY3214996 for 48 h at 37˚C.

Reverse transcription-quantitative PCR (RT-qPCR). Total RNA was extracted using an RNeasy micro kit (Qiagen GmbH). Reverse transcription was performed using the Mir-X miRNA First-Strand Synthesis kit (Clontech Laboratories, Inc.), according to the manufacturer's instructions. The mixture was incubated for 1 h at 37˚C and then terminated at 85˚C for 5 min. RNA levels were quantified using a CFX Connect RT PCR detection system (Bio-Rad Laboratories, Inc.) and SYBR Green PCR Master Mix (Toyobo Life Science). The reaction mixture consisted of 1.0 μg cDNA, 9 μl SYBR-Green Mix and 10 μmol each primer. GAPDH was used as the reference mRNA control, while U6 was the reference miRNA control. The thermocycling conditions consisted of an initial denaturation at 95˚C for 10 min, followed by 40 cycles at 95˚C for 15 sec, 58˚C for 30 sec and 72˚C for 40 sec. The following PCR primer sets were used: Alkaline phosphatase (ALP) sense, 5'-ACTGCAGACATTCTCAAAGC-3' and antisense, 5'-GAGTGAGTGAGTGAGCAAGG-3' (15); Runx2 sense, 5'-ATGCTTCATTCGCCTCAC-3' and antisense, 5'-ACTGCTTGCAGCCTTAAAT-3' (16); Notch2 sense, 5'-CCCTGGGCTACACTGGGAAAAACTG-3' and antisense, 5'-GGCAGGGGTTGGACGCACACTCA-3' (17); GAPDH sense, 5'-GTGAACCATGAGAAGTATGACAA-3' and antisense, 5'-ATGAGTCCTTCCACGATACC-3' (18); miR-181c-5p sense, 5'-GGGAACATTCAACCTGTCG-3' and antisense, 5'-GTGCGTGTCGTGGAGTCG-3' (19); and U6 sense, 5'-GCTTCGGCAGCACATATACTAAAAT-3' and antisense, 5'-CGCTTCACGAATTTGCGTGTCAT-3' (19). The quantification of mRNA expression relative to an internal control, GAPDH, was performed by the $2^{-\Delta\Delta Cq}$ method (20). The results are expressed as the mean ± SD of three independent experiments.

Western blotting. Mammalian Cell Lysis kit (Sigma-Aldrich; Merck KGaA) was used to prepare protein extracts. Protein concentrations were determined using a protein assay kit (Bio-Rad Laboratories, Inc.). Protein (10 μg) samples were solubilized by boiling in sample buffer, then separated by 10% SDS-PAGE and transferred to a nitrocellulose membrane. The membrane was blocked with Blocking One-P reagent (Nacalai Tesque, Inc.) for 1 h at room temperature. After incubation with the primary antibody at room temperature overnight, immunoblots were labeled with a horseradish peroxidase-conjugated secondary antibody for 1 h at room temperature Bands on western blots were detected using an enhanced chemiluminescence western blotting reagent (Cytiva). Images were captured with a cooled charge-coupled device (CCD) camera system (LAS-4000; Fujifilm Wako Pure Chemical Corporation). Antibodies used for western blotting were as follows: i) Anti-human Runx2 mouse monoclonal (1:1,000; cat. no. 8486; Cell Signaling Technology); ii) anti-human ERK1/2 rabbit monoclonal (1:1,000; cat. no. 4695; Cell Signaling Technology, Inc.); iii) anti-human phosphorylated (p)-ERK1/2 rabbit monoclonal (1:1,000; cat. no. 9101; Cell Signaling Technology, Inc.); iv) anti-human Notch2 rabbit monoclonal (1:1,000; cat. no. 4530; Cell Signaling Technology); v) anti-human GAPDH mouse monoclonal (1:1,000; cat. no. MAB374; EMD Millipore Corporation); vi) horseradish peroxidase-conjugated sheep anti-mouse antibody (1:1,000; cat. no. NA931; Cytiva); vii) horseradish peroxidase-conjugated donkey anti-rabbit antibody (1:1,000; cat. no. NA934; Cytiva). ImageJ version 1.47 (National Institutes of Health) was used for densitometric scanning of the protein bands. G3PDH expression was used as an internal control. Protein expression levels were normalized

to GAPDH signals. Data are presented as the mean ± SD of three independent experiments.

Immunofluorescence. Cells were fixed with 4% paraformaldehyde in PBS for 1 h at room temperature, permeabilized using 0.2% Triton X-100 in PBS for 5 min at room temperature and then blocked with PBS + 5% FBS (Biological Industries) for 1 h at room temperature. The samples were incubated with Alexa Fluor® 488-conjugated anti-Runx2 rabbit monoclonal antibody (Abcam; 1:1,000; cat. no. ab215954 in PBS + 1% BSA [Sigma-Aldrich; Merck KGaA]) for 60 min at room temperature. Then, Alexa Fluor® 568 phalloidin (Thermo Fisher Scientific, Inc.; 1:500) was used to stain F-actin. Slides were rinsed in PBS, mounted in DAPI Fluoromount-G (SouthernBiotech) and examined using a Biorevo BZ-9000 fluorescence microscope (Keyence Corporation), magnification, x400.

Small interfering (si) RNA knockdown. Stealth™ siRNA for Notch2 (si Notch2; 5'-GAGCACCUGUGAGAGGAAUAUU GAU-3' and 5'-AUCAAUAUUCCUCUCACAGGUGCUC-3') and negative control (si control; cat. no. 12935112; both from Thermo Fisher Scientific, Inc.) were used for Notch2 knockdown experiments. Cells were transfected with siRNA (10 nM) using HiPerFect transfection reagent (Qiagen GmbH) for 48 h according to the manufacturer's instructions. Subsequent experiments were performed immediately after 48 h of siRNA transfection.

Transfection of miRNA inhibitor and miRNA mimics. Cells were transfected with miRNA inhibitor or miRNA mimics for miR-181c-5p using Lipofectamine® RNAiMAX Transfection reagent (Thermo Fisher Scientific, Inc.), in accordance with the manufacturer's instructions. Cells were transfected with miRNA inhibitor or miRNA mimics for 48 h. mirVana™ miRNA inhibitors (cat. no. 4464084), inhibitor negative controls (cat. no. 4464076), mimics (cat. no. 4464066) and mimics negative controls (cat. no. 4464058) were each used at a final concentration of 10 nM. All transfection reagents and miRNAs were from Thermo Fisher Scientific, Inc. Subsequent experiments were performed immediately after 48 h of transfection.

ALP enzyme activity. ALP enzyme activity was examined using a TRACP and ALP Assay kit (Takara Bio, Inc.; cat. no. MK301). After 7 days of culture in osteoblastic differentiation medium, cells were homogenized in the provided extraction solution and sonicated for 3 min. Cell lysates were collected and assayed in accordance with the manufacturer's instructions. The absorbance at 405 nm was detected using a microplate reader (Bio-Rad Laboratories, Inc.), as a measure of ALP activity. The data are presented as the mean ± SD of three independent experiments.

Alizarin Red staining and quantification. Alizarin red staining was performed as described in our previous study (10). The cells were fixed in 10% neutral buffered formalin (Sigma-Aldrich; Merck KGaA) at room temperature. After 30 min, formalin was aspirated and the cells were washed with deionized distilled water. Alizarin Red solution (1.0%) was added and incubated at room temperature in the dark for 1 h. Light microscopy was used to visualize the specimens (magnification, x40). Quantitation of Alizarin red staining was performed by measuring the absorbance of dissolved alizarin red. Cell monolayers were submerged in 20% methanol and 10% acetic acid solution in water. The spectrophotometric absorbance of the samples was measured at 405 nm using a microplate reader. The results are expressed as the mean ± SD of three independent experiments.

Microarray analysis of miRNA expression. The Affymetrix GeneChip miRNA 4.0 array was used for miRNA expression analysis. Microarray analysis was performed using 1 μg total RNA labeled with the FlashTag™ Biotin HSR RNA Labeling kit in accordance with the manufacturer's instructions. Biotin-labeled samples were hybridized on the GeneChip miRNA microarray, according to the manufacturer's instructions. The array was then washed with GeneChip™ Wash Buffer and stained using the Genechip Fluidics Station 450, and scanned using the GeneChip Scanner. Raw data were extracted automatically with the Affymetrix data extraction protocol, using the Transcriptome Analysis Console Software version 4.0 (Thermo Fisher Scientific, Inc.). CEL file importing, miRNA expression Robust Multi-array Average (RMA)+Detected Above Background (DABG)-All analysis, and result exporting were performed using Affymetrix Power Tools Software version 2.11.2 For significant differentially expressed miRNAs (DEmiRNA), hierarchical cluster analysis was conducted using complete linkage and Euclidean distance as a measure of similarity (21,22). All reagents, kits and software were from Affymetrix (Thermo Fisher Scientific, Inc.).

Identification of potential targets for miRNA. TargetScan v7.2 (http://www.targetscan.org) was used to identify potential miRNA targets in the 3'-untranslated region (UTR) of candidate genes. TargetScan can predict biological targets of miRNAs by searching for the presence of conserved sites that match the sequence of each miRNA (23). Predictions are ranked based on the predicted efficacy of targeting, as calculated using context scores of the sites in mammals (24).

Statistical methods. Data were expressed as the mean ± SD. Data were analyzed statistically using SPSS software (version 24; IBM Corp.). Tukey's Honestly Significant Difference test was used for multiple comparisons. Statistical analysis was otherwise performed using unpaired Student's t-test. $P<0.05$ was considered to indicate a statistically significant difference.

Results

MEL induces osteogenic differentiation of hOB cells. hOB cells displayed spindle-like morphology in the absence of osteogenic induction medium. hOB cells exhibited positive alizarin red staining after they had been cultured in osteogenic induction medium (Fig. 1A). These observations suggested that primary hOB cells derived from mandibular bone exhibited osteogenetic characteristics *in vitro*. Therefore, the effect of MEL on osteogenetic characteristics was investigated in hOB

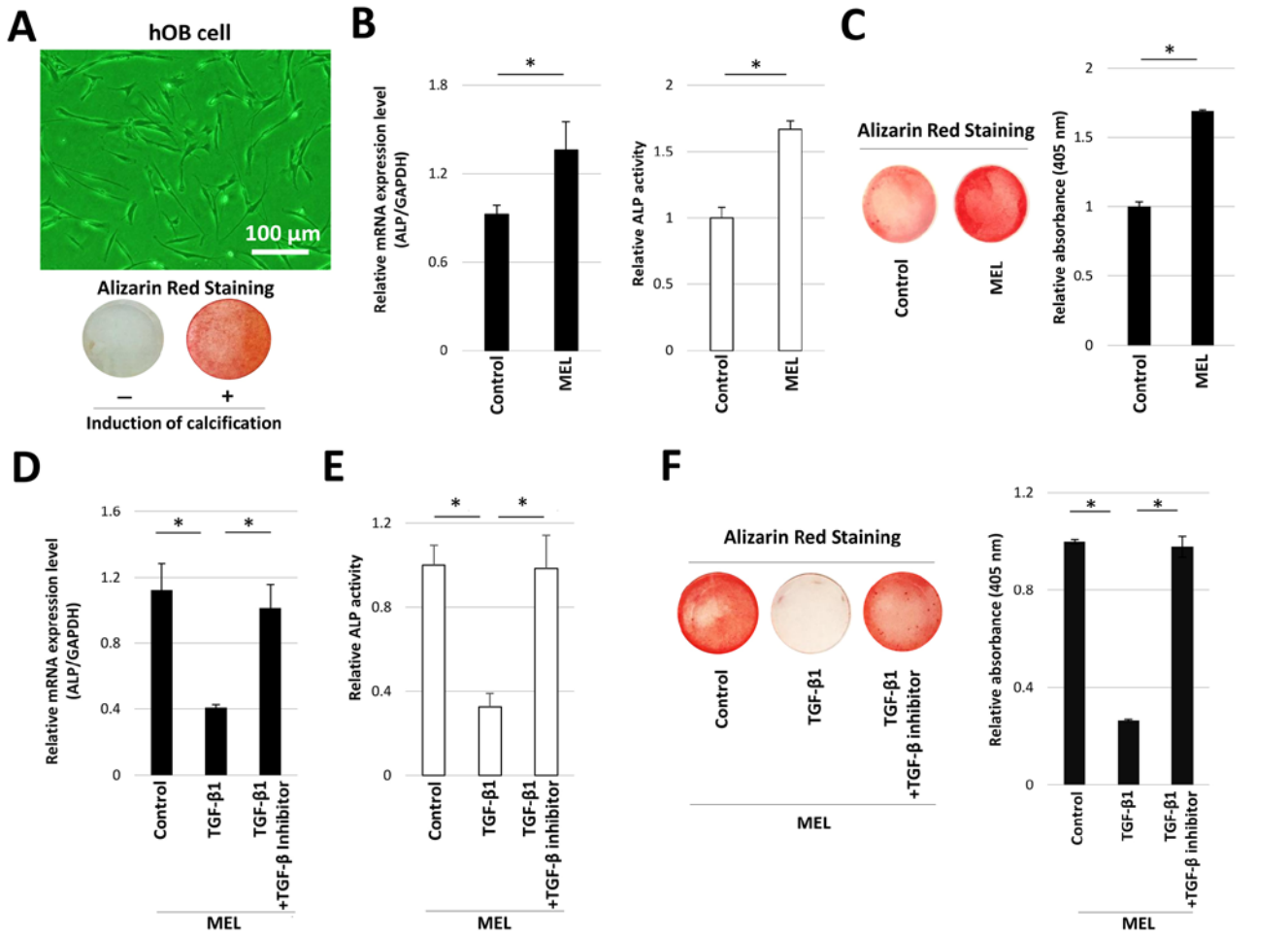

Figure 1. MEL-induced calcification in hOB cells is attenuated by TGF-β1 treatment. (A) Morphology of hOB cells. hOB cells presented spindle-like morphology in the absence of osteogenic induction medium. hOB cells exhibited positive alizarin red staining after they had been cultured in osteogenic induction medium. Scale bar, 100 μm. (B) ALP mRNA expression and ALP enzyme activity in the presence of MEL. (C) Representative images of Alizarin red staining and relative absorbance of hOB cells cultured in the presence MEL. (D) ALP mRNA expression, (E) ALP enzyme activity and (F) relative absorbance of Alizarin red staining in hOB cells cultured in the presence of MEL, together with TGF-β1 or TGF-β1 and TGF-β inhibitor. *P<0.05. MEL, melatonin; hOB, human jawbone-derived osteoblast-like; ALP, alkaline phosphatase; TGF-β1, transforming growth factor-β1.

cells. The level of mineralization staining was highest in the presence of 1.0 μM MEL. Furthermore, mineralization staining in hOB cells was significantly enhanced in the presence of 1.0 μM MEL, compared with untreated controls (Fig. S1). Therefore, 1.0 μM MEL was used in the present study. MEL treatment significantly enhanced ALP mRNA expression and enzyme activity, compared with control cells (Fig. 1B). Alizarin red staining was also performed on hOB cells treated with MEL for 14 days in osteogenic induction medium, and it was identified that treatment with MEL resulted in significantly greater mineralization staining, compared with control cells (Fig. 1C). These results indicated that MEL could promote calcification in hOB cells.

The effect of TGF-β1 on MEL-induced mineralization was also investigated. Treatment with 5 ng/ml TGF-β1 significantly inhibited MEL-induced ALP mRNA expression and activity (Fig. 1D and E). However, concomitant treatment with TGF-β1 and TGF-β inhibitor restored ALP expression and enzymatic activity, reaching similar levels to control cells. MEL-induced mineralization was also attenuated by treatment with TGF-β1, which was restored following co-treatment with TGF-β inhibitor (Fig. 1F).

MEL-induced upregulation of Runx2 expression in hOB cells is reduced by treatment with TGF-β1. Runx2 mRNA and protein expression levels were significantly increased in the presence of MEL alone (Fig. 2A-C). However, MEL-induced upregulation of Runx2 expression was significantly inhibited by TGF-β1 treatment, and this effect was reversed by treatment with TGF-β inhibitor. Immunofluorescence staining identified that Runx2 protein was present in the nucleus cell. It was found that treatment with TGF-β1 reduced the numbers of Runx2-positive cells, but this reduction was reversed by treatment with a TGF-β inhibitor (Fig. 2D).

MEL-induced Runx2 expression is reduced by ERK1/2 activation. The effects of TGF-β1 treatment on the phosphorylation levels of ERK1/2 were evaluated using western blot analysis (Fig. 3A). The levels of p-ERK1/2 were determined by normalizing the densities of p-ERK1/2 bands to total ERK1/2. Treatment with TGF-β1 significantly enhanced the phosphorylation levels of ERK1/2 (Fig. 3B). Western blotting of p-ERK1/2 was performed in the addition of ERK inhibitor to check whether ERK inhibitor can block ERK1/2 pathway by inhibition of phosphorylation levels of ERK1/2. ERK1/2 phosphorylation was significantly

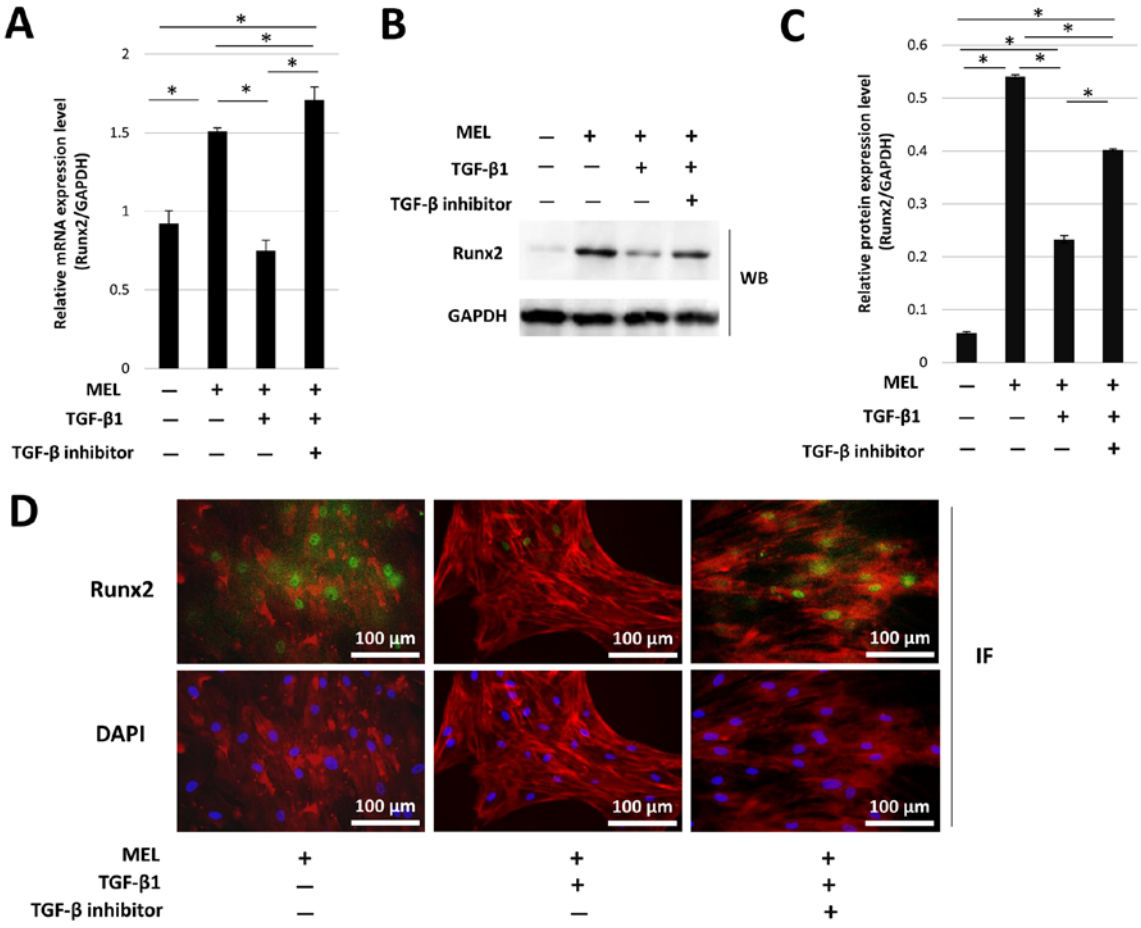

Figure 2. MEL-induced Runx2 expression in hOB cells is reduced by TGF-β1 treatment. Runx2 (A) mRNA expression, (B) protein expression and (C) protein densitometry in hOB cells in the presence of MEL. (D) Immunofluorescence of Runx2 (green), F-actin (red) and DAPI nuclear staining (blue). Magnification, x400. Scale bar, 100 μm. *P<0.05. MEL, melatonin; hOB, human jawbone-derived osteoblast-like; TGF-β1, transforming growth factor-β1; WB, western blotting; IF, immunofluorescence; Runx2, RUNX family transcription factor 2.

reduced in TGF-β1-treated hOB cells following the addition of an ERK inhibitor (Fig. S2A and B). Furthermore, the effect of ERK inhibitor treatment on Runx2 expression was assessed following treatment with MEL and TGF-β1. Compared with MEL and TGF-β1-treated cells, the addition of ERK inhibitor significantly increased the TGF-β1-inhibited Runx2 mRNA and protein expression, as well as the levels of mineralization staining (Fig. 3C-F).

MEL-induced Runx2 upregulation and calcification is mediated by miR-181c-5p. Microarray analysis was performed to investigate the effect of MEL on miRNA expression in hOB cells. In total, 124 miRNAs were differentially expressed in MEL-treated hOB cells, compared with untreated cells. Of these DEmiRNAs, 17 were upregulated (>2-fold increase), while 13 were downregulated (<0.5-fold reduction). The upregulated and downregulated miRNAs are summarized in Tables I and II, respectively. Of the upregulated miRNAs, miR-181c-5p exhibited the greatest upregulation and was therefore selected for subsequent experiments.

The effects of miR-181c-5p inhibition were investigated. miR-181c-5p inhibitor-transfected hOB cells exhibited significantly lower expression of miR-181c-5p, compared with cells transfected with inhibitor control (Fig. 4A). ALP and Runx2 mRNA expression levels were then determined in hOB cells transfected with miR-181c-5p inhibitor in the presence of MEL. Transfection with miR-181c-5p inhibitor significantly reduced Runx2 and ALP mRNA expression levels (Fig. 4B), as well as mineralization staining in the presence of MEL (Fig. 4C).

The effect of miR-181c-5p overexpression on ALP and Runx2 mRNA expression levels was also examined using miR-181c-5p mimic transfection. miR-181c-5p expression was significantly increased in hOB cells transfected with miR-181c-5p mimics, compared with mimics control (Fig. 5A). Transfection with miR-181c-5p mimics resulted in a significant upregulation in Runx2 and ALP mRNA expression levels, compared with mimics control (Fig. 5B). Similarly, mineralization staining was also significantly enhanced (Fig. 5C). These results suggested that Runx2 expression and mineralization were dependent on miR-181c-5p expression.

Notch2 expression is reduced by miR-181c-5p overexpression. Using TargetScan, position 2,967-2,974 within the 3'-UTR of the Notch2 gene was identified as a putative binding site for miR-181c-5p (Fig. 6A). Notch2 has been reported to serve a significant role in the regulation of osteoblastic cell differentiation (25). Therefore, the role of miR-181c-5p in regulation of Notch2 expression was examined. Notch2 mRNA and protein expression levels were significantly reduced in hOB

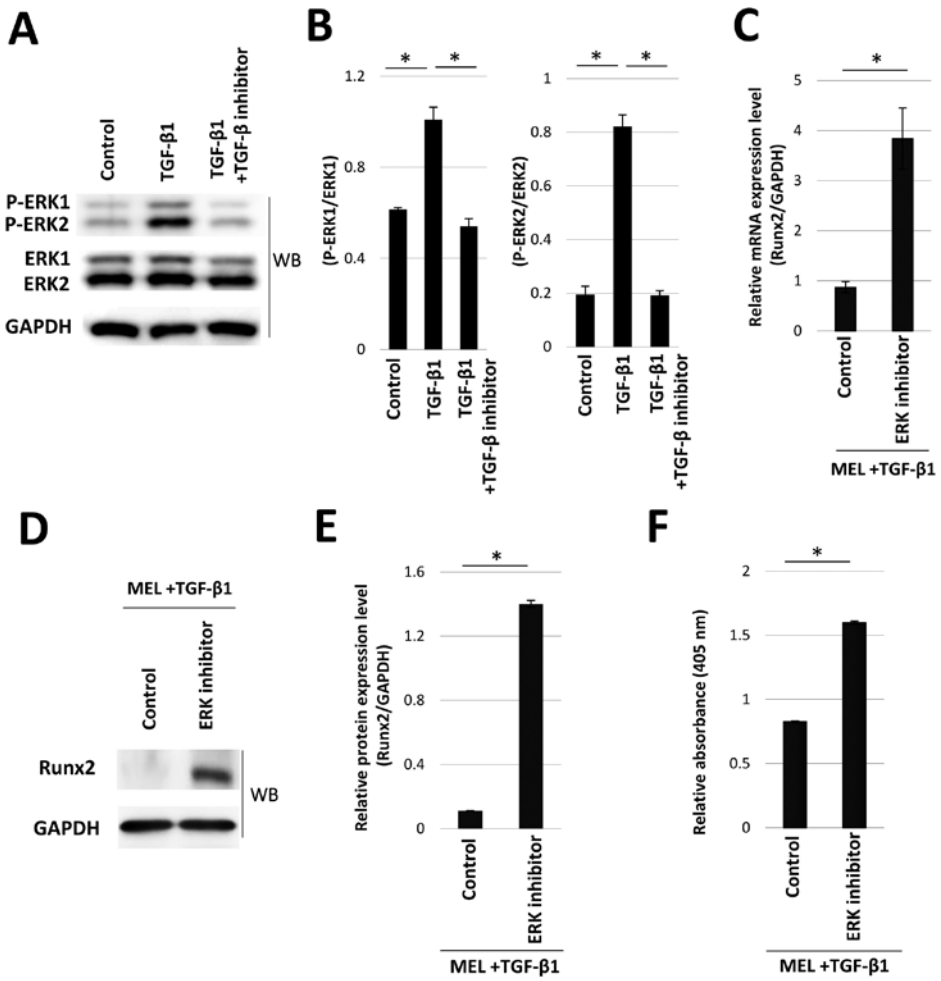

Figure 3. MEL-induced Runx2 expression is attenuated by TGF-β1-induced ERK1/2 activation. (A) WB images and (B) densitometry of p-ERK1/2 levels in the presence of TGF-β1 or TGF-β1 + TGF-β inhibitor. (C) Runx2 mRNA expression, (D) WB of Runx2, (E) Runx2 protein expression and (F) relative absorbance of mineralization staining in ERK inhibitor-treated hOB cells in the presence of MEL and TGF-β1. *P<0.05. MEL, melatonin; hOB, human jawbone-derived osteoblast-like; TGF-β1, transforming growth factor-β1; p-, phosphorylated; WB, western blotting; Runx2, RUNX family transcription factor 2.

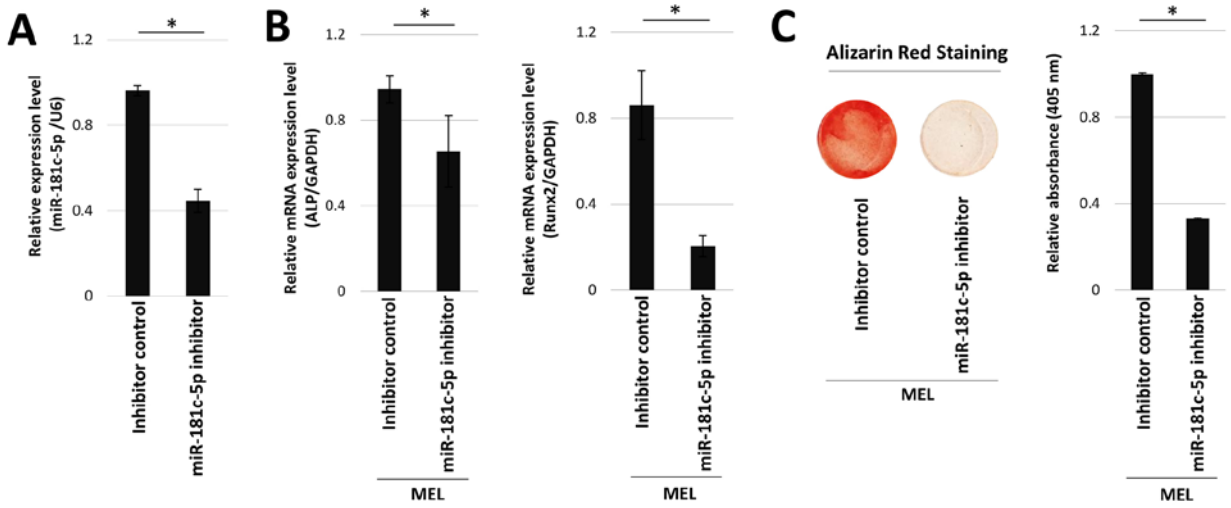

Figure 4. Runx2 expression and mineralization in hOB cells is reduced by miR-181c-5p inhibition. (A) miR-181c-5p expression, (B) ALP and Runx2 mRNA expression levels and (C) relative absorbance of mineralization staining in hOB cells following transfection with miR-181c-5p inhibitor and MEL treatment. *P<0.05. MEL, melatonin; hOB, human jawbone-derived osteoblast-like; miR, microRNA; Runx2, RUNX family transcription factor 2; ALP, alkaline phosphatase.

cells transfected with miR-181c-5p mimics, compared with mimics control (Fig. 6B and C). The association between Notch2 and Runx2 was then determined using Notch2 siRNA silencing. Transfection with si Notch2 significantly reduced

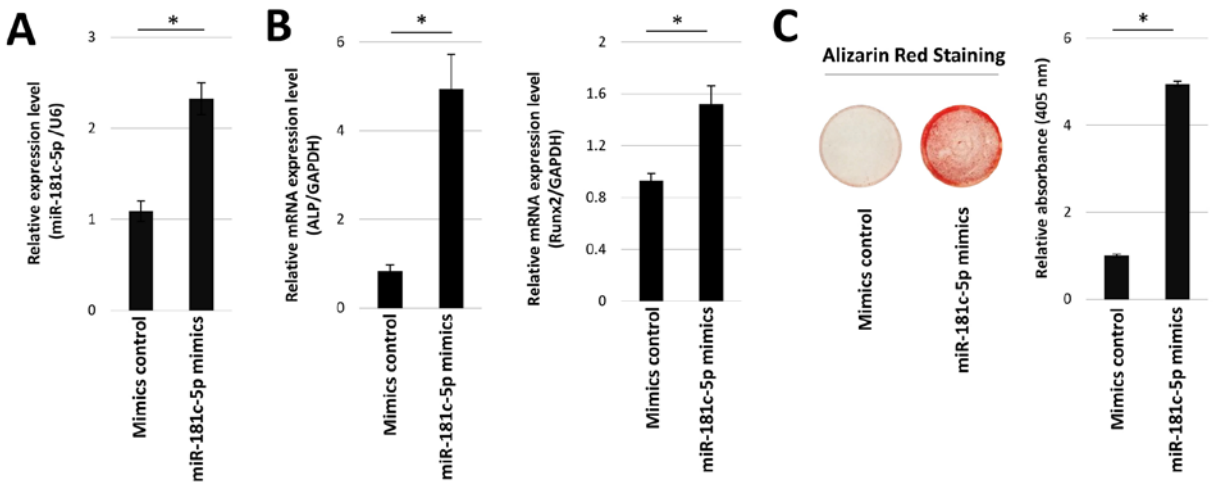

Figure 5. Overexpression of miR-181c-5p increases Runx2 expression and mineralization. (A) miR-181c-5p expression, (B) ALP and Runx2 mRNA expression levels and (C) relative absorbance of mineralization staining in human jawbone-derived osteoblast-like cells following transfection with miR-181c-5p mimics. *P<0.05. MiR, microRNA; ALP, alkaline phosphatase; Runx2, RUNX family transcription factor 2.

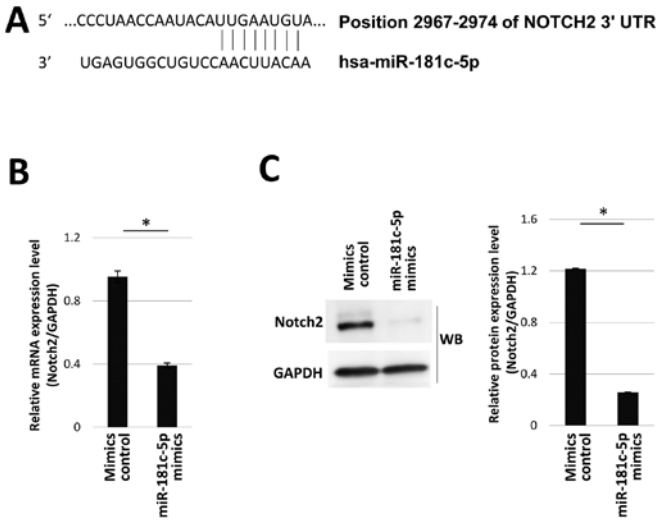

Figure 6. miR-181c-5p overexpression reduces Notch2 expression. (A) Putative miR-181c-5p binding site in the Notch2 3'-UTR. Notch2 (B) mRNA and (C) protein expression in human jawbone-derived osteoblast-like cells transfected with miR-181c-5p mimics. *P<0.05. miR, microRNA; ALP, alkaline phosphatase; WB, western blotting; UTR, untranslated region; Runx2, RUNX family transcription factor 2.

Table I. miRNAs upregulated in melatonin-treated human jawbone-derived osteoblast-like cells.

miRNA	Fold change
miR-181c-5p	4.57
miR-1973	3.99
miR-501-3p	3.64
miR-4788	3.25
miR-654-3p	2.92
miR-642a-3p	2.77
miR-5195-3p	2.68
miR-4800-5p	2.61
miR-188-5p	2.54
miR-3195	2.39
miR-8089	2.33
miR-30a-3p	2.30
miR-4743-5p	2.19
miR-3135b	2.12
miR-3651	2.04
miR-505-3p	2.02
miR-30d-5p	2.01

miR/miRNA, microRNA.

Notch2 mRNA and protein expression levels, compared with si control (Fig. 7A and B). Moreover, Notch2 knockdown significantly increased Runx2 mRNA and protein expression levels (Fig. 7C and D), as well as mineralization staining (Fig. 7E).

Discussion

The object of the present study was to assess the role of MEL in mineralization and the effect of TGF-β on osteoblastic cell differentiation in human osteoblastic cells. It has been reported that MEL induces the differentiation of mesenchymal cells and preosteoblasts into mature osteoblastic cells (6-8). MEL also induces mineralization of mouse osteoblastic cells via the BMP/ERK/Wnt signaling pathway (11) and promotes the proliferation of human osteoblastic cells via ERK1/2 activation (26). In the present study, treatment with MEL enhanced the expression of Runx2, an important regulatory factor for hOB cell differentiation and mineralization (27). These results suggested that MEL could serve as an important regulator of osteogenic differentiation and mineralization in osteoblastic cells.

miRNAs are known to regulate key biological processes, including cell proliferation, differentiation and death (28-30). Additionally, miRNAs are likely to serve positive or negative roles in osteoblast differentiation via the regulation of target

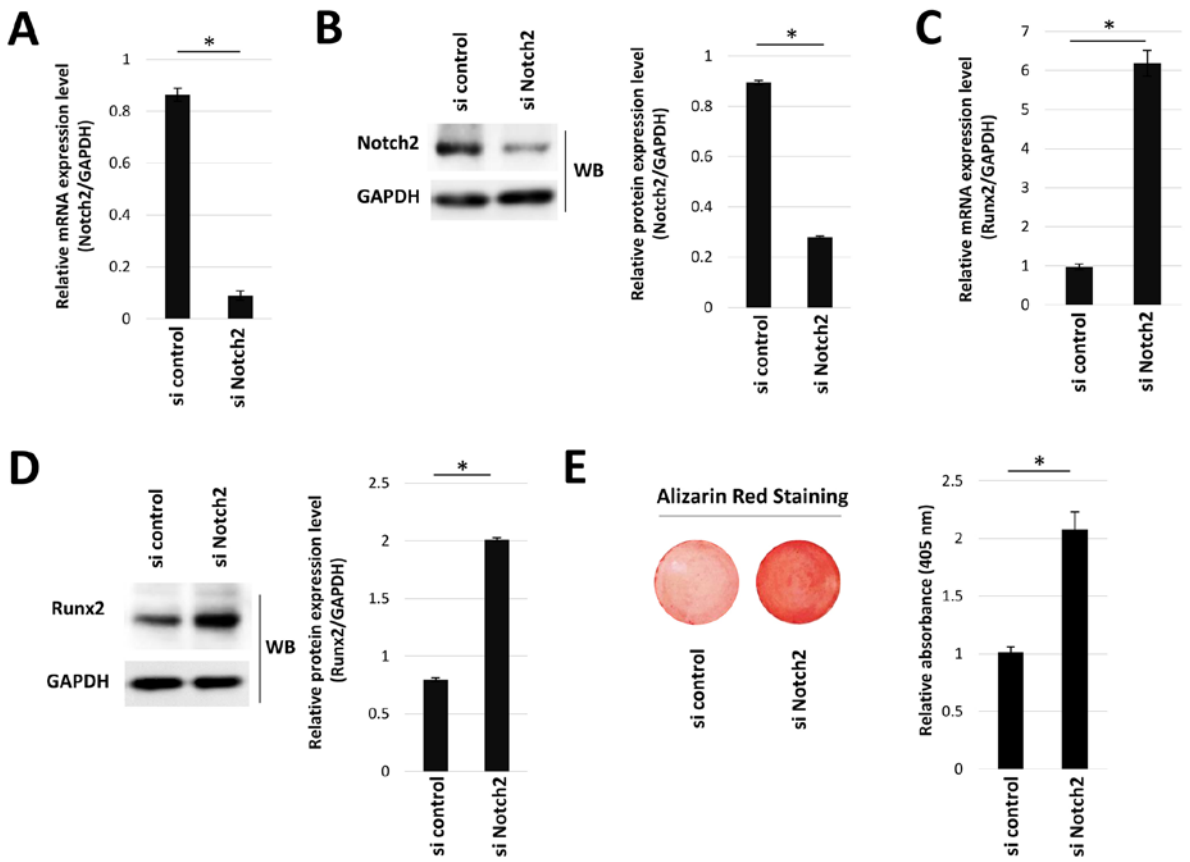

Figure 7. Runx2 expression is increased by Notch2 knockdown. Notch2 (A) mRNA and (B) protein expression in hOB cells transfected with si Notch2. Runx2 (C) mRNA and (D) protein expression in hOB cells transfected with si Notch2. (E) Relative absorbance of mineralization staining in hOB cells transfected with si Notch2. *P<0.05. WB, western blotting; hOB, human jawbone-derived osteoblast-like; si, small interfering.

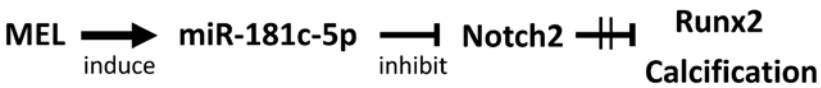

Figure 8. Proposed model for the role of MEL in human osteoblast differentiation. MEL-induced expression of miR-181c-5p enhances both Runx2 expression and calcification via Notch2 inhibition in human osteoblastic cells. MEL, melatonin; miR, microRNA; Runx2, RUNX family transcription factor 2.

Table II. miRNAs downregulated in melatonin-treated human jawbone-derived osteoblast-like cells.

miRNA	Fold change
miR-4663	0.235
miR-3148	0.291
miR-6740-5p	0.308
miR-5189-5p	0.332
miR-548x-3p	0.363
miR-181a-2-3p	0.383
miR-3180-3p	0.401
miR-16-2-3p	0.415
miR-21-3p	0.465
miR-1281	0.483
miR-1247-3p	0.489
miR-212-3p	0.499
miR-6782-5p	0.499

miR/miRNA, microRNA.

gene expression and modulation of cell signaling pathways. For instance, some miRNAs are involved in the regulation of osteogenic differentiation in osteoblastic cells via direct or indirect targeting of Runx2 (31). Moreover, miR-590-5p enhances osteogenic differentiation in mouse mesenchymal stem cells by indirectly stabilizing Runx2 expression (32). In the present study, MEL-induced expression of miR-181c-5p promoted Runx2 expression and calcification in hOB cells. To the best of our knowledge, this is the first report demonstrating a role for miR-181c-5p expression in human osteoblastic cell differentiation.

In the current study, Notch2 was identified as a potential target of miR-181c-5p in hOB cells. However, whether Notch2 transcription is directly suppressed by miR-181c-5p activity remains unknown. Thus, further studies are required to elucidate the specific mechanism via which Notch2 expression is modulated by miR-181c-5p. It has been reported that miR-758 regulates bone-related gene expression and bone formation via the inhibition of Notch2 in periodontal ligament stem cells (33). The results of the present study are consistent with these findings and support the importance of miRNA in the regulation of

Notch2 expression, thus controlling bone formation and mineralization. Furthermore, in the present study, Notch2 silencing enhanced both Runx2 expression and calcification in hOB cells. These results suggested that MEL-induced expression of miR-181c-5p may promote human osteogenic differentiation via the suppression of Notch2-dependent signaling. The Notch signaling pathway is involved in osteoblast differentiation (25). Notably, Notch2 suppresses osteoblastic cell differentiation and bone formation (34,35). The Notch/recombination signal binding protein for immunoglobulin κJ region/Hey signaling pathway is suggested to affect osteoblast differentiation via the inhibition of Runx2 and nuclear factor of activated T cells c1 in mice (34). Moreover, Notch3 attenuates Runx2 expression and osteogenic differentiation in bone marrow-derived mesenchymal stem cells (36). These findings suggest that Notch signaling negatively regulates osteogenic differentiation via the suppression of Runx2 expression.

The effect of TGF-β on osteoblast differentiation remains controversial. For instance, whether TGF-β facilitates or inhibits osteoblast differentiation and bone formation it yet to be elucidated. The concentration of TGF-β and stage of osteoblast differentiation may influence osteogenic differentiation and bone formation (37-39). In addition, cell proliferation, chemotaxis and early differentiation of osteoprogenitor cells are promoted by TGF-β/Smad signaling (12). In contrast, the TGF-β/Smad signaling pathway also inhibits osteoblast maturation, mineralization and transition to the osteocyte cell type (12).

TGF-β can activate the MAPK/ERK pathway and inhibit osteogenesis in pluripotent mesenchymal cells (C3H10T1/2 cell line), as well as in preosteoblastic cells (MC3T3 cell line) (13). The MAPK/ERK signaling pathway may also serve a predominant role in mouse osteogenic differentiation (13). In the present study, MEL-induced Runx2 expression and mineralization were attenuated by TGF-β1-induced ERK1/2 activation in hOB cells. This observation indicated that osteogenic differentiation could be inhibited by TGF-β-induced ERK activation in human osteoblastic cells.

In conclusion, MEL regulates the expression of miR-181c-5p in hOB cells, which in turn may enhance both Runx2 expression and mineralization via Notch2 downregulation (Fig. 8). The present findings indicated that MEL serves an important role in the modulation of miR-181c-5p expression and supports the osteogenic differentiation of human osteoblastic cells. However, it remains to be elucidated whether miR-181c-5p can directly inhibit Notch2 transcription. Further studies are required to elucidate the specific role of the Notch2-dependent signaling pathway in Runx2 expression and osteogenic differentiation.

Acknowledgements

Not applicable.

Funding

The present work was supported by a Grant-in-aid for Scientific Research (grant no. 18K09790) from the Ministry of Education, Culture, Sports, Science and Technology of Japan.

Availability of data and materials

All data generated or analyzed in this study are included in this published article.

Authors' contributions

HM performed experiments and analyzed and interpreted the data. HS designed the study, analyzed and interpreted the data, and wrote the paper. HK, SY and MS performed experiments. MTad, SO and MZR discussed, analyzed and interpreted the data. KO and MTak designed the study and aided in writing the paper. All authors read and approved the final manuscript.

Ethics approval and consent to participate

The present study was approved by the Ethical Committee of Hiroshima University (approval no. E-930). Bone fragments were obtained from a patient who underwent mandibular osteotomy and had provided written informed consent for use of the fragments in this study.

Patient consent for publication

Not applicable.

Competing interests

The authors declare that they have no competing interests.

References

1. Singh M and Jadhav HR: Melatonin: Functions and ligands. Drug Discov Today 19: 1410-1418, 2014.
2. Reiter RJ, Tan DX, Rosales-Corral S and Manchester LC: The universal nature, unequal distribution and antioxidant functions of melatonin and its derivatives. Mini Rev Med Chem 13: 373-384, 2013.
3. Conti A, Conconi S, Hertens E, Skwarlo-Sonta K, Markowska M and Maestroni JM: Evidence for melatonin synthesis in mouse and human bone marrow cells. J Pineal Res 28: 193-202, 2000.
4. Liu C, Fukuhara C, Wessel JH III, Iuvone PM and Tosini G: Localaization of Aa-nat mRNA in the rat retina: Melatonin synthesis by florescence in situ hybridization and laser capture microdissection. Cell Tissue Res 315: 197-201, 2004.
5. Salehi B, Sharopov F, Fokou PVT, Kobylinska A, Jonge L, Tadio K, Sharifi-Rad J, Posmyk MM, Martorell M, Martins N, *et al*: Melatonin in medicinal and food plants: Occurrence, bioavailability, and health potential for humans. Cells 8: E681, 2019.
6. Roth JA, Kim BG, Lin WL and Cho MI: Melatonin promotes osteoblast differentiation and bone formation. J Biol Chem 274: 22041-22047, 1999.
7. Ostrowska Z, Ziora K, Kos-Kudła B, Swietochowska E, Oświecimska J, Dyduch A, Wołkowska-Pokrywa K and Szapska B: Melatonin, the RANKL/RANK/OPG system, and bone metabolism in girls with anorexia nervosa. Endokrynol Pol 61: 117-123, 2010.
8. Sethi S, Radio NM, Kotlarczyk MP, Chen CT, Wei YH, Jockers R and Witt-Enderby PA: Determination of the minimal melatonin exposure required to induce osteoblast differentiation from human mesenchymal stem cells and these effects on downstream signaling pathways. J Pineal Res 49: 222-238, 2010.
9. Takechi M, Tatehara S, Satomura K, Fujisawa K and Nagayama M: Effect of FGF-2 and melatonin on implant bone healing: A histomorphometric study. J Mater Sci Mater Med 19: 2949-2952, 2008.
10. Rahman MZ, Shigeishi H, Sasaki K, Ota A, Ohta K and Takechi M: Combined effects of melatonin and FGF-2 on mouse preosteoblast behavior within interconnected porous hydroxyapatite ceramics - in vitro analysis. J Appl Oral Sci 24: 153-161, 2016.

11. Park KH, Kang JW, Lee EM, Kim JS, Rhee YH, Kim M, Jeong SJ, Park YG and Kim SH: Melatonin promotes osteoblastic differentiation through the BMP/ERK/Wnt signaling pathways. J Pineal Res 51: 187-194, 2011.
12. Wu M, Chen G and Li YP: TGF-β and BMP signaling in osteoblast, skeletal development, and bone formation, homeostasis and disease. Bone Res 4: 16009, 2016.
13. Sun X, Xie Z, Ma Y, Pan X, Wang J, Chen Z and Shi P: TGF-β inhibits osteogenesis by upregulating the expression of ubiquitin ligase SMURF1 via MAPK-ERK signaling. J Cell Physiol 233: 596-606, 2018.
14. Huang C, Geng J and Jiang S: MicroRNAs in regulation of osteogenic differentiation of mesenchymal stem cells. Cell Tissue Res 368: 229-238, 2017.
15. Nettelhoff L, Grimm S, Jacobs C, Walter C, Pabst AM, Goldschmitt J and Wehrbein H: Influence of mechanical compression on human periodontal ligament fibroblasts and osteoblasts. Clin Oral Investig 20: 621-629, 2016.
16. Lu Z, Wang G, Roohani-Esfahani I, Dunstan CR and Zreiqat H: Baghdadite ceramics modulate the cross talk between human adipose stem cells and osteoblasts for bone regeneration. Tissue Eng Part A 20: 992-1002, 2014.
17. Dallas DJ, Genever PG, Patton AJ, Millichip MI, McKie N and Skerry TM: Localization of ADAM10 and Notch receptors in bone. Bone 25: 9-15, 1999.
18. Hashikata M, Shigeishi H, Okui G, Yamamoto K, Tobiume K, Seino S, Uetsuki R, Kato H, Ishioka Y, Ono S, *et al*: Snail-induced CD44(high) cells in HNSCC with high ABC transporter capacity exhibit potent resistance to cisplatin and docetaxel. Int J Clin Exp Pathol 9: 7908-7918, 2016.
19. Gao ZQ, Wang JF, Chen DH, Ma XS, Yang W, Zhe T and Dang XW: Long non-coding RNA GAS5 antagonizes the chemoresistance of pancreatic cancer cells through down-regulation of miR-181c-5p. Biomed Pharmacother 97: 809-817, 2018.
20. Livak KJ and Schmittgen TD: Analysis of relative gene expression data using real-time quantitative PCR and the 2(-ΔΔC(T)) method. Methods 25: 402-408, 2001.
21. Gerstein M and Jansen R: The current excitement in bioinformatics-analysis of whole-genome expression data: How does it relate to protein structure and function? Curr Opin Struct Biol 10: 574-584, 2000.
22. Quackenbush J: Computational analysis of microarray data. Nat Rev Genet 2: 418-427, 2001.
23. Lewis BP, Burge CB and Bartel DP: Conserved seed pairing, often flanked by adenosines, indicates that thousands of human genes are microRNA targets. Cell 120: 15-20, 2005.
24. Agarwal V, Bell GW, Nam JW and Bartel DP: Predicting effective microRNA target sites in mammalian mRNAs. eLife 4: e05005, 2015.
25. Regan J and Long F: Notch signaling and bone remodeling. Curr Osteoporos Rep 11: 126-129, 2013.
26. Xiong XC, Zhu Y, Ge R, Liu LF and Yuan W: Effect of melatonin on the extracellular-regulated kinase signal pathway activation and human osteoblastic cell line hFOB 1.19 proliferation. Int J Mol Sci 16: 10337-10353, 2015.
27. Gomathi K, Akshaya N, Srinaath N, Moorthi A and Selvamurugan N: Regulation of Runx2 by post-translational modifications in osteoblast differentiation. Life Sci 245: 117389, 2020.
28. Zhao Y and Srivastava D: A developmental view of microRNA function. Trends Biochem Sci 32: 189-197, 2007.
29. Le MT, Xie H, Zhou B, Chia PH, Rizk P, Um M, Udolph G, Yang H, Lim B and Lodish HF: MicroRNA-125b promotes neuronal differentiation in human cells by repressing multiple targets. Mol Cell Biol 29: 5290-5305, 2009.
30. Körner C, Keklikoglou I, Bender C, Wörner A, Münstermann E and Wiemann S: MicroRNA-31 sensitizes human breast cells to apoptosis by direct targeting of protein kinase C epsilon (PKCepsilon). J Biol Chem 288: 8750-8761, 2013.
31. Narayanan A, Srinaath N, Rohini M and Selvamurugan N: Regulation of Runx2 by MicroRNAs in osteoblast differentiation. Life Sci 232: 116676, 2019.
32. Vishal M, Vimalraj S, Ajeetha R, Gokulnath M, Keerthana R, He Z, Partridge NC and Selvamurugan N: MicroRNA-590-5p stabilizes Runx2 by targeting Smad7 during osteoblast differentiation. J Cell Physiol 232: 371-380, 2017.
33. Peng W, Deng W, Zhang J, Pei G, Rong Q and Zhu S: Long noncoding RNA ANCR suppresses bone formation of periodontal ligament stem cells via sponging miRNA-758. Biochem Biophys Res Commun 503: 815-821, 2018.
34. Tu X, Chen J, Lim J, Karner CM, Lee SY, Heisig J, Wiese C, Surendran K, Kopan R, Gessler M, *et al*: Physiological notch signaling maintains bone homeostasis via RBPjk and Hey upstream of NFATc1. PLoS Genet 8: e1002577, 2012.
35. Yu W, Jiang D, Yu S, Fu J, Li Z, Wu Y and Wang Y: SALL4 promotes osteoblast differentiation by deactivating NOTCH2 signaling. Biomed Pharmacother 98: 9-17, 2018.
36. Wang H, Jiang Z, Zhang J, Xie Z, Wang Y and Yang G: Enhanced osteogenic differentiation of rat bone marrow mesenchymal stem cells on titanium substrates by inhibiting Notch3. Arch Oral Biol 80: 34-40, 2017.
37. Zhang H, Ahmad M and Gronowicz G: Effects of transforming growth factor-beta 1 (TGF-beta1) on in vitro mineralization of human osteoblasts on implant materials. Biomaterials 24: 2013-2020, 2003.
38. Alliston T, Choy L, Ducy P, Karsenty G and Derynck R: TGF-beta-induced repression of CBFA1 by Smad3 decreases cbfa1 and osteocalcin expression and inhibits osteoblast differentiation. EMBO J 20: 2254-2272, 2001.
39. Kaji H, Naito J, Sowa H, Sugimoto T and Chihara K: Smad3 differently affects osteoblast differentiation depending upon its differentiation stage. Horm Metab Res 38: 740-745, 2006.